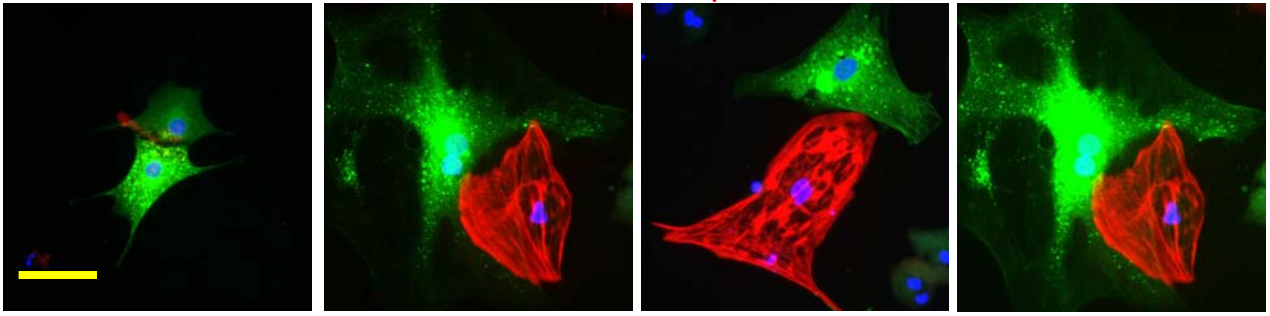
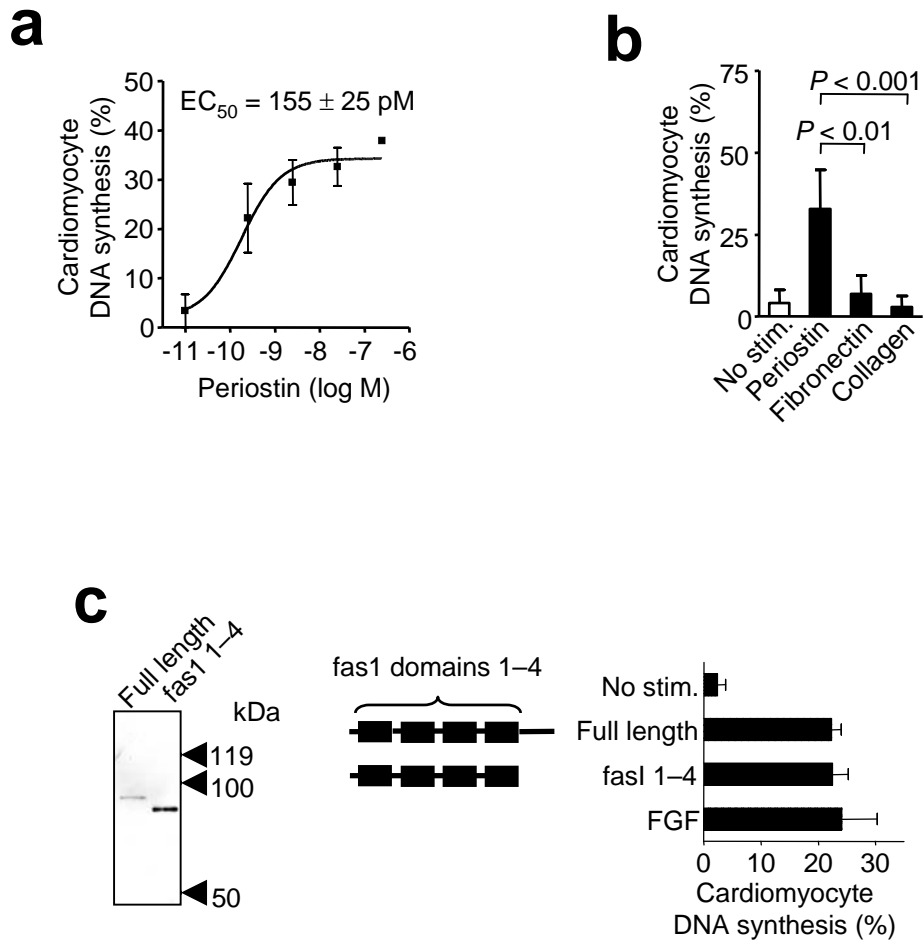


Supplementary Figure 1. Periostin induces proliferation of neonatal cardiomyocytes. **a**, Primary neonatal rat ventricular cardiomyocytes were stimulated for 3 days and cell cycle activity was quantified by immunofluorescence microscopy. **b**, Additive effect of periostin and FGF on DNA synthesis. **c**, Proliferating fraction determined by expression of marker Ki67. **d**, Cardiomyocyte proliferation determined by cell count. **e**, Inactivation of cell cycle inhibitor retinoblastoma protein determined with antibody against phosphorylated retinoblastoma protein (P-Rb). **f**, Nuclear accumulation of cell cycle activator cyclin A. Scale bars, 50 μ m; Color codes given at the top. Data are means \pm SEM of 3 independent experiments. Statistical significance tested by ANOVA and t-test.

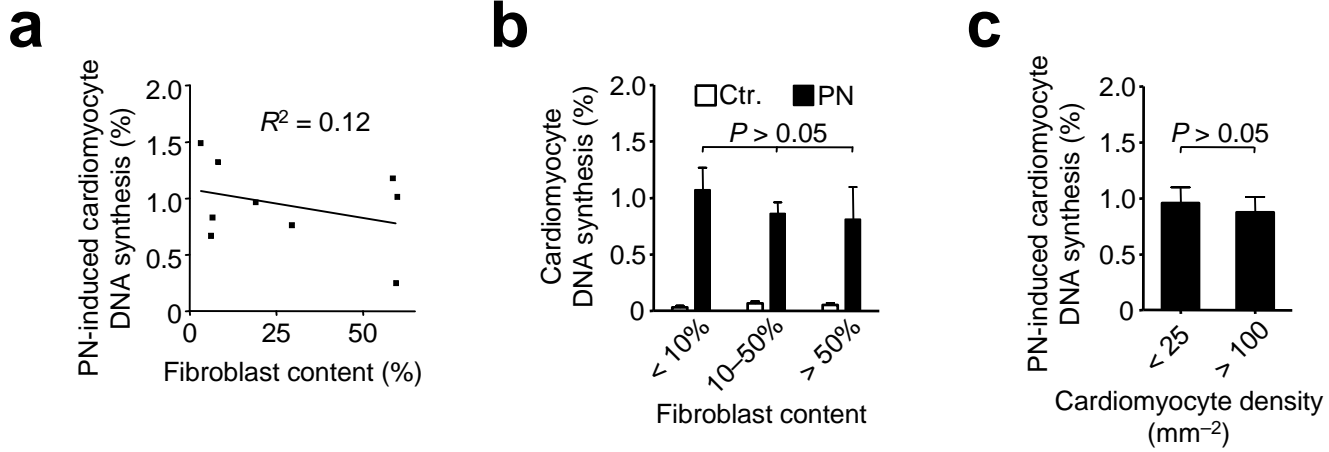
GFP, DAPI, troponin I



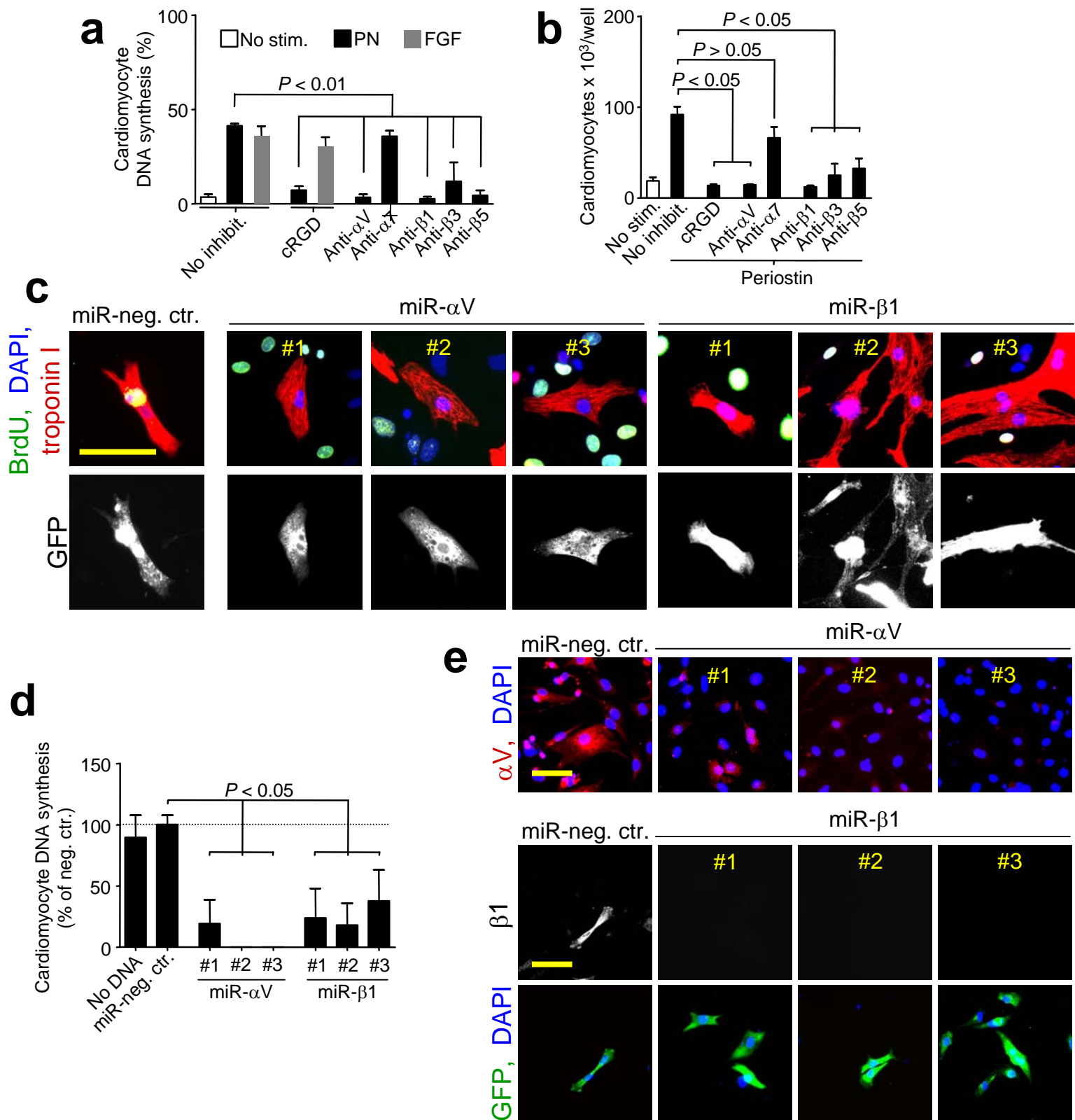
Supplementary Figure 2. Cardiac fibroblasts form cell-cell contacts with differentiated cardiomyocytes, but do not fuse to induce cell cycle re-entry *in vitro*. Isolated adult rat ventricular cardiomyocytes were co-cultured for 9 days with autologous cardiac fibroblasts genetically labeled by infection with a third generation lentivirus directing expression of GFP under control of the CMV promoter. Representative samples depicting cell-cell contact between cardiomyocytes and cardiac fibroblasts without fusion are shown. Color code given at the top. Scale bar, 50 μm .



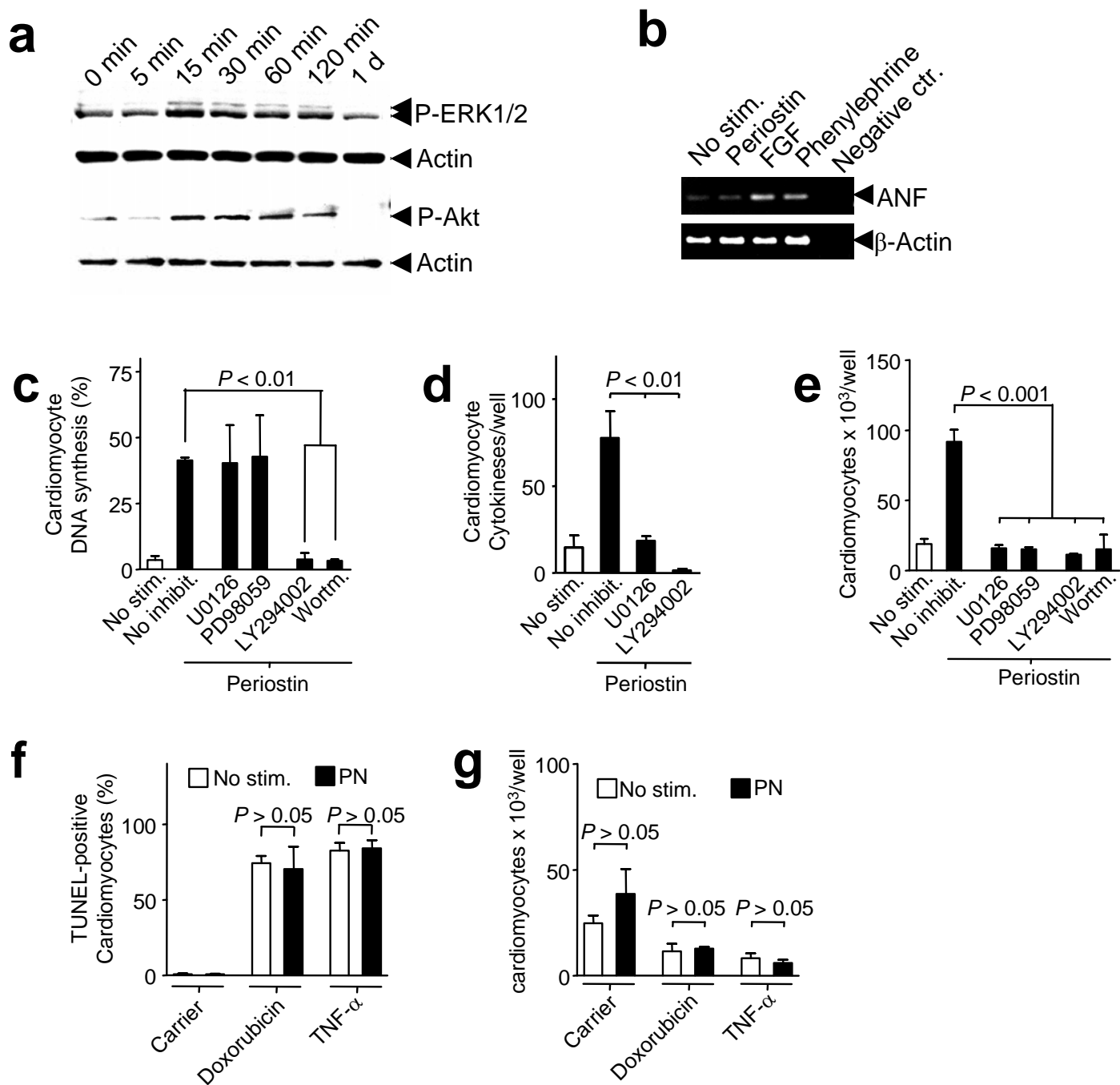
Supplementary Figure 3. Periostin-stimulated cardiomyocyte proliferation is specific and requires the periostin fas1 domains. Assays were performed in primary neonatal rat ventricular cardiomyocytes. **a**, DNA synthesis in the presence of increasing concentrations of periostin. **b**, Cardiomyocyte DNA synthesis in the presence of periostin, fibronectin, or collagen type I. **c**, Recombinant full length periostin and fas1 1-4 domains analyzed by Western blot and by stimulation of DNA synthesis. No stim., no stimulation; Statistical significance tested with ANOVA.



Supplementary Figure 4. Periostin-induced cardiomyocyte cell cycle re-entry does not correlate with abundance of cardiac fibroblasts. Assays were performed in isolated adult rat ventricular cardiomyocytes. **a, b**, Isolated adult rat ventricular cardiomyocytes were seeded with different amounts of autologous cardiac fibroblasts. Periostin-induced cardiomyocyte DNA synthesis was determined by immunofluorescence microscopy. **a**, Regression of periostin-induced cardiomyocyte DNA synthesis and percentage of fibroblasts present in the same specimen shows lack of correlation. **b**, Cardiomyocyte cell cycle re-entry in the absence and presence of periostin and different percentages of autologous cardiac fibroblasts. **c**, Isolated adult rat ventricular cardiomyocytes were seeded at different densities and periostin-induced cardiomyocyte cell cycle re-entry was determined by immunofluorescence microscopy. Ctr., control; PN, periostin.



Supplementary Figure 5. Periostin-stimulated proliferation of neonatal cardiomyocytes requires integrins. Periostin-induced DNA synthesis (**a**) and proliferation (**b**) of neonatal ventricular cardiomyocytes is blocked by cRGD (10 μM) and integrin blocking antibodies (10 $\mu\text{g}/\text{mL}$). **c**, Suppression of periostin-induced cardiomyocyte BrdU uptake with microRNA (miR) sequences targeting integrin αV and $\beta 1$ (number of construct indicated in each panel). **d**, Quantification of periostin-induced BrdU-uptake after transduction with different targeting constructs. Dotted line indicates periostin-induced cardiomyocyte DNA synthesis in the presence of miR-negative control. **e**, Suppression of integrin αV and $\beta 1$ expression by miR constructs (number of construct indicated in each panel). Color codes given on the left. Scale bars, 50 μm . No stim., no stimulation; PN, periostin; No inhibit., no inhibitor; cRGD, cyclic RGD peptide; miR-neg.ctr., hairpin structure predicted not to target any known vertebrate gene; Statistical significance tested with ANOVA.



Supplementary Figure 6. Periostin-stimulated proliferation of neonatal cardiomyocytes requires ERK1/2 and PI3-kinase. **a**, Stimulation with periostin (duration of stimulation indicated at the top) followed by visualization of ERK1/2 and Akt phosphorylation by Western blot. Membranes re-probed with an antiserum against actin (lower panels). **b**, Transcription of atrial natriuretic factor (ANF) determined by RT-PCR with β -actin as positive control. **c–e**, Cardiomyocyte DNA synthesis (**c**), cytokinesis (**d**), and proliferation (**e**) inhibited by ERK inhibitors U0126 (10 μ M) and PD98059 (1 μ M) or PI3-kinase inhibitors LY294002 (10 μ M) and Wortmannin (0.1 μ M). **f**, Determination of cardiomyocyte apoptosis by TUNEL assay. **g**, Determination of cardiomyocyte survival. Data are means \pm SEM representative for 3 independent experiments. No stim., no stimulation; PN, periostin; Statistical significance tested with ANOVA.

Supplementary Information

Periostin Induces Proliferation of Differentiated Cardiomyocytes and Promotes Cardiac Repair

Bernhard Kühn, Federica del Monte, Roger J. Hajjar, Yuh-Shin Chang,

Djamel Lebeche, Shima Arab, and Mark T. Keating

Supplementary Methods

Supplementary Table 1. Periostin improves ventricular remodeling and function after myocardial infarction.

Supplementary Table 2. Summary of recently published protocols to induce therapeutic cardiomyocyte proliferation.

Supplementary Table 3. Image acquisition, editing, and analysis.

Supplementary Table 4. Details of quantitative microscopic analyses.

Supplementary References

Supplementary Methods

Materials. Recombinant periostin, purified from HEK293 cells expressing the full-length human cDNA, was provided by Drs. Lan-Bo Chen and Meiru Dai (DFCI, Boston, MA)¹. The polypeptide consisting of the fas1 domains 1–4 of human periostin was purified from bacteria and was provided by BioVendor. FGF1 and NRG-1 β were provided by R&D Systems. The antibodies against integrin α V (RMV-7) and β 1 (HM β 1-1) were provided by BioLegend. The antibody against integrin α 7 (6A11) was provided by MBL. The antibodies against integrin β 3 (F11), β 5 (MAB1961Z), and against aurora B kinase were provided by BD Biosciences. Rat fibronectin was from Biomedical Technologies. The Akt $\frac{1}{2}$ inhibitor and phenylephrine were provided by Sigma and all other chemical inhibitors were provided by BD Biosciences. The antibodies against tropomyosin (CH1) and troponin T (CT3) were provided by the Developmental Studies Hybridoma Bank. Antibodies against human periostin and 5-Bromo-2'-deoxyuridine (BrdU) were provided by AbCam. The antibodies against troponin I, MEF-2, vWF, and c-kit were provided by Santa Cruz Biotechnology. The antibody against smooth muscle actin (1A4) was provided by Sigma and the antibody against phosphorylated histone H3 was provided by Upstate. Fluorophore-conjugated secondary antibodies raised in goat were provided by Invitrogen.

Cardiomyocyte isolation and culture. Primary neonatal rat ventricular cardiomyocytes were isolated using the Neomyts kit (Cellutron), seeded at a density of 10^5 cells/cm² onto gelatin-coated cover slips, stimulated for 3 days, and labeled with BrdU for the terminal 2 days.

Neonatal cardiomyocyte proliferation, survival, and apoptosis. To determine cardiomyocyte proliferation, primary neonatal rat ventricular cardiomyocytes were quantified by counting with a hemocytometer after 3 days and 6 days of stimulation. Corresponding samples were stained with an antibody directed against tropomyosin as a cardiomyocyte marker to control for the percentage of differentiated cardiomyocytes. To determine cardiomyocyte survival, primary neonatal rat ventricular cardiomyocytes were pre-treated with 500 ng/mL periostin or buffer for 30 min and then exposed to 0.5 μ M doxorubicin or 100 ng/mL TNF- α for 24 hr and quantified by counting. Apoptotic cardiomyocyte nuclei were determined after 24 hr with the In situ Cell Death Detection Kit (Roche) in combination with staining for troponin I.

Transcriptional analysis. Complementary DNA was synthesized from 2 μ g RNA with the SuperScriptIII kit (Invitrogen) using oligo-dT primers. One μ L cDNA was used as template for 20 μ L PCR-reactions (95 $^{\circ}$ C for 2 min, 30 cycles of 95 $^{\circ}$ C for 30 sec, 55 $^{\circ}$ C for 30 sec, 72 $^{\circ}$ C for 1 min, followed by 72 $^{\circ}$ C for 10 min). Oligonucleotide primers used for detection of β -MHC were F: 5'-CTTCAACCACCACATGTTCG-3', R: 5'-TACAGGTGCATCAGCTCCAG-3'; SMA F: 5'-GTCGGTATGGGTCAGAAGGA-3', R: 5'-CTTTTCCAGGGAGGAGGAAG-3'; SERCA2 F: 5'-ACTGGTGATGGTGTGAACGA-3', R: 5'-TACGGGGACTCAAAGATTGC-3', ANF F: 5'-ATACAGTGCGGTGTCCAACA-3', R: 5'-GGATCTTTTGGCATTCTGCTC-3', β -actin F: 5'-GGAGAAGATTTGGCACCACAC-3', R: 5'-CAGGGAGGAAGAGGATGCGGC-3', and for GAPDH: 5'-CTCATGACCACAGTCCATGC-3', R: 5'-ATGTAGGCCATGAGGTCCAC-3'.

Immunofluorescence microscopy. DNA-synthesis was analyzed by visualization of BrdU uptake and mitosis by visualization of mitotic nuclei with condensed chromosomes with an antibody against phosphorylated histone H3. Cytokinesis was determined by detection of the cleavage furrow and the midbody with an antibody against aurora B kinase. Signals were visualized with secondary antibodies conjugated to Alexa 488, Alexa 546, Alexa 594, and Alexa 647 (Invitrogen). Nuclei were visualized with 4',6'-diamidino-2-phenylindole (DAPI, Invitrogen). For image acquisition, the value for γ was set at 1 and the lookup table settings were linear (details of image acquisition in **Supplementary Table 3** online).

Determination of cardiomyocyte cell cycle activity and cardiac regeneration *in vivo*. Horizontal cryosections of 14 μ m thickness spaced at 1 mm intervals were analyzed by laser scanning immunofluorescence microscopy. BrdU-positive cardiomyocyte nuclei and cytokineses were quantified on 16–20 sections per heart. Fibrosis and cardiomyocyte cross-sectional area were determined on 5 Masson's Trichrome-stained sections per heart at the level of the injection at 40x magnification and quantified using the Metamorph software package (Molecular Devices Corp.). For cell cycle analysis of single cardiomyocytes, they were isolated, plated, and fixed. An antibody directed against phosphorylated histone H3 (Upstate) was used to visualize cycling cardiomyocytes.

Preparation of recombinant periostin. Recombinant periostin was purified from HEK293 cells expressing the full-length human cDNA¹. The periostin fas1-

only polypeptide purified from *E. coli* was provided by BioVendor. Purity of >90% was established by SDS-PAGE and Coomassie staining.

RNAi suppression of integrin α V and β 1 subunits. Oligonucleotides directed against the coding sequences of α V and β 1 integrin subunits were subcloned into the mammalian expression vector pcDNA 6.2-GW/EmEGFP-miR (Block-IT Pol II miR RNAi Expression Vector Kit, Invitrogen). The following oligonucleotides

coding for pre-microRNA were used: α V #1: 5'-TGCTGTTAGCTTGACACCTGC GTCTTGT TTTGGCCACTGACTGACAAGACGCATGTCAAGCTAA-3', α V #2: 5'-T GCTGTTGAGTTCCAGCCTTCATCGGGTTTTGGCCACTGACTGACCCGATGAA CTGGA ACTCAA-3', α V #3: 5'-TGCTGTTGCCTTGCTGAATGAACTTGGTTTTGG CCACTGACTGACCAAGTTCACAGCAAGGCAA-3', β 1 #1: 5'-TGCTGATTCCTT GTAAACAGGCTGGAGTTTTGGCCACTGACTGACTCCAGCCTTTACAAGGAAT- 3', β 1 #2: 5'-TGCTGTTTCCAGACAGTGTGCCCACTGTTTTGGCCACTGACTGA CAGTGGGCACTGTCTGGAAA-3', β 1 #3: 5'-TGCTGTGAAGGACCACCTCTACT TCTGTTTTGGCCACTGACTGACAGAAGTAGGTGGTCCTTCA-3'. Two μ g of plasmid DNA was electroporated (Amaza Inc.) into 5×10^6 freshly isolated neonatal rat ventricular cardiomyocytes. Transduction efficiency determined by expression of GFP was $31.9 \pm 10.9\%$ ($n = 6$). Stimulation was begun 36 hr later and periostin-induced cardiomyocyte cell cycle re-entry was determined as described above. Transduced cardiomyocytes identified by GFP-expression were scored for analysis. Suppression of integrin protein levels was determined by immunofluorescence microscopy using antibodies against integrin α V (Chemicon) and against β 1 (BD Pharmingen).

Western blot of myocardial tissue. Heart tissue was lysed in 20 mM Tris (pH 7.5), 150 mM NaCl, 10 mM EDTA, 1 mM EGTA, 1% Triton X-100, 2.5 mM sodium pyrophosphate, 1 mM β -glycerol phosphate, 1 mM Na_3VO_4 , 1 g/mL leupeptin, 1% NP-40 and 0.24 mg/mL Pefabloc SC (Roche) at 4 C. Protein concentrations were determined using the BCA assay (Pierce). Forty μ g of cell lysate was separated on 10% SDS-polyacrylamide gels, blotted onto nitrocellulose membranes (Amersham), which were then incubated with antibodies according to manufacturer's directions, followed by visualization with ECL reagent (Amersham).

Analysis of myocardial regeneration. Horizontal cryosections of 14 μ m thickness spaced at 1 mm intervals were analyzed. To determine infarct size, Masson's Trichrome-stained sections were analyzed at 1x magnification. The infarct border zone was defined as myocardial tissue within 0.5 mm of the fibrous scar tissue. Fibrosis and cardiomyocyte cross-sectional area were determined after staining with Masson's Trichrome at 10x and 40x magnification, respectively, and quantified using the Metamorph software package. BrdU-positive cardiac fibroblast nuclei were determined at 5 cross-sections per heart at the level of the myocardial infarction. Cardiomyocyte nuclei were counted using the optical dissector method² on troponin T and DAPI-stained sections in 32 – 60 random sample volumes of 84,500 μm^3 per heart. BrdU-positive cardiomyocyte nuclei were quantified on 16–20 sections per heart. Cardiomyocyte apoptosis was determined using the *In situ* Cell Death Detection Kit (Roche) in combination with staining for troponin I. Capillaries, arterioles, and stem cells were detected with antibodies against von Willebrand

factor (vWF), smooth muscle actin (SMA), and c-kit, respectively, and quantified at the level of the myocardial infarction.

Supplementary Table 1. Perioestin improves ventricular remodeling and function after myocardial infarction. Summary of echocardiography and catheterization results. Means were compared by ANOVA.

Echocardiography	Control (<i>n</i> = 8)		Perioestin (<i>n</i> = 9)		<i>P</i> between groups at 12 weeks
	1 week	12 weeks	1 week	12 weeks	
Shortening fraction (%)	22.9 ± 1.5	22.6 ± 1.8	25.2 ± 2.1	33.0 ± 2.6	0.006
<i>P</i>	0.7		<0.0001		
Ejection fraction (%)	51.1 ± 2.5	50.2 ± 3.2	52.6 ± 2.9	65.9 ± 3.8	0.006
<i>P</i>	0.6		0.0023		
End-diastolic dimension (mm)	8.1 ± 0.6	10.3 ± 0.4	8.1 ± 0.4	8.4 ± 0.2	0.02
<i>P</i>	0.0086		0.07		
End-systolic dimension (mm)	6.4 ± 0.4	7 ± 0.6	6.1 ± 0.4	6 ± 0.5	> 0.05
<i>P</i>	0.2		0.9		
Catheterization	Control (<i>n</i> = 8)		Perioestin (<i>n</i> = 7)		
	1 week	12 weeks	1 week	12 weeks	
Slope of end-systolic pressure-volume relationship (mm Hg/ L)	ND	0.5 ± 0.01	ND	1.4 ± 0.2	0.003
Preload-recruitable stroke work (mm Hg)	ND	13.9 ± 5	ND	68.6 ± 13.9	
Maximum rate of left ventricular pressure rise (mm Hg/s)	ND	3225 ± 170	ND	4821 ± 513	0.01
Maximum left ventricular elastance	ND	0.6 ± 0.01	ND	2.5 ± 1	

Supplementary Table 2. Summary of recently published protocols to induce therapeutic cardiomyocyte proliferation.

	Cyclin D2³	P193/p53⁴	Cyclin A2⁵	FGF/p38i⁶	Periostin
Species	Mouse	Mouse	Rat	Rat	Rat
Intervention	α MHC-cyclin D2 transgene	α MHC-p53 dominant negative x α MHC-p190 dominant negative, transgene transcription beginning postnatal day 5	Adenoviral gene transfer of cyclin A2 under control of CMV-promoter	1 intramyocardial injection of FGF, 1 month intraperitoneal injection of p38 inhibitor	Local delivery of recombinant periostin for 3 months
Cardiomyocyte cycling in absence of injury	Increased	Increased	Increased ⁷	Increased ⁸	Increased
Injury model	Permanent LAD ligation	Permanent LAD ligation	Permanent LAD ligation	Permanent LAD ligation	Permanent LAD ligation
Cardiomyocyte cell cycle activity (border zone)	Early	1 week: 1% DNA synthesis (1 injection ³ H-Thy)	6 weeks: 4.4% DNA synthesis (4 injections BrdU), 4.6% proliferating fraction (Ki-67), 1.2% mitosis (H3P)	2 weeks: 0.3% mitosis (H3P)	1 week: 0.6% DNA synthesis (3 injections BrdU), 0.18% mitosis (H3P)
	Late	5 months: 0.5% DNA synthesis (1 injection ³ H-Thy)		4 weeks: 0.5% DNA synthesis (1 injection ³ H-Thy)	3 months: no mitoses (H3P)
Echocardiography: control -> treatment	ND	ND	ND	FS: 39% -> 50% EF: ND	FS: 23% -> 33% EF: 50% -> 66%
Catheterization	ND	ND	Improved ESPVR, compliance	ND	Improved ESPVR, compliance
Circumferential infarct size: ctr -> treatment	56% -> 36%	ND	ND	29% -> 14%	36% -> 19%

Legend to Supplementary Table 2: CMV, cytomegalovirus; ND, not done; LAD, left anterior descending coronary artery; ³H-Thy, ³H-Thymidine; H3P, phosphorylated histone H3; FS, fractional shortening; EF, ejection fraction; ESPVR, end-systolic pressure-volume relationship.

Supplementary Table 3. Image acquisition, editing, and analysis.

Acquisition Settings		
	Hardware	Software and settings
Fig. 1a, b	Axioplan 2 Epifluorescence microscope ¹ , 40x lens (PlanNeofluar)	Axiocam ¹ , Axiovision ¹ , 200-600 msec exposure, 1,300x1,300 px, 8 bit
Fig. 1d, e	Olympus IX-81 epifluorescence microscope ² with LUCPLFL 40x and UPLFL 10x lenses equipped with Hamamatsu CM CCD camera	10-100 msec exposure, 12 bit, IP lab 4 ²
Fig. 2e	Axioplan 2 Epifluorescence microscope ¹ , 40x lens (PlanNeofluar)	Axiocam ¹ , Axiovision ¹ , 200-600 msec exposure, 1,300x1,300 px, 8 bit
Fig. 2g	BioDoc-It System ³	1 - 2 sec exposure
Fig. 3a, d	Olympus IX-81 epifluorescence microscope ² with LUCPLFL 40x and UPLFL 10x lenses equipped with Hamamatsu CM CCD camera	10-100 msec exposure, 12 bit, IP lab 4 ²
Fig. 3e, f, g	Fluoview 1000 laser scanning confocal microscope ² with 60x S-Achromat lens, confocal aperture 125 μ m, step width for confocal stacks 0.3 μ m	Fluoview software Vers. 1.4a ² , 2 s/px, zoom 2, 1,024x1,024 px, Argon laser for 488 nm, He/Ne laser for 594 nm and 647 nm Reslicing in xz plane: Fluoview 3D software Vers. 1.4a
Fig. 4b	Fluoview 1000 laser scanning confocal microscope ² with 60x S-Achromat lens, confocal aperture 125 μ m	Fluoview software Vers. 1.4a ² , 2 s/px, zoom 2, 1,024x1,024 px, Argon laser for 488 nm, He/Ne laser for 594 nm and 647 nm
Fig. 4c	Kodak BioMax Light Film ⁴	2 sec – 1 min exposure
Fig. 4f, g	Millar catheter SPR-838, Power Lab [®] DAQ System ⁵	200 Hz sampling rate, PVAN3.3 software ⁵
Fig. 5a	Leica MCFL III ⁶ with Plan Apo 1x lens equipped with AxioCam MRC Carl Zeiss ¹	AxioVision ¹ , 89-165 msec exposure, 1,300x1,030 px, 12 bit
Fig. 5b, h	Axioplan 2 microscope ¹ , 40x lens (PlanNeofluar)	Axiocam ¹ , Axiovision ¹ , 200-600 msec exposure, 1,300x1,300 px, 8 bit
Fig. 6a, c, f	Fluoview 1000 laser scanning confocal microscope ² with 40x and 60x S-Achromat lens	Fluoview software Vers. 1.4a ² , 2 s/px, zoom 2, 1,024x1,024 px, Argon laser for 488 nm, He/Ne laser for 594 nm and 647 nm
Fig. 6e, g	Olympus IX-81 epifluorescence microscope ² with LUCPLFL 40x lens equipped with Hamamatsu CM CCD camera	10-100 msec exposure, 12 bit, IP lab 4 ²

Legend to Supplementary Table 3. Key to manufacturers: ¹ Carl Zeiss Inc.,

Thornwood, NY; ² Olympus America Inc. Melville, NY; ³ UVP, Upland, CA; ⁴

Eastman Kodak Company, Rochester, NY; ⁵ Millar Instruments, Inc., Houston, TX; ⁶ Leica Microscopy Systems Ltd, Heerbrugg, Switzerland;

Supplementary Table 4. Details of quantitative microscopic analyses.

Figure	Number of cardiomyocytes, nuclei, and hearts analyzed
Fig. 1a	15,001 cardiomyocytes
Fig. 1b	9,625 cardiomyocytes
Fig. 1d	58 cardiomyocytes in cytokinesis
Fig. 1e	115,648 cardiomyocytes
Fig. 3g	BrdU-uptake: 439,150 nuclei Cytokinesis: 313,679 nuclei
Fig. 3h	18,803 cardiomyocytes
Fig. 6b	BrdU-uptake: 1 week: 62,649 12 weeks: 502,467 Apoptosis: 1 week: 68,010 12 weeks: 100,493
Fig. 6c	1 week: 34,009 12 weeks: 272,768
Fig. 6d	1 week: 234 12 weeks: 2,005

Supplementary References

1. Tai, I.T., Dai, M. & Chen, L.B. Periostin induction in tumor cell line explants and inhibition of in vitro cell growth by anti-periostin antibodies. *Carcinogenesis* **26**, 908–915 (2005).
2. Howard, C.V. & Reed, M. *Unbiased Stereology: Three-Dimensional Measurement In Microscopy*, (BIOS Scientific Publishers, Oxford, 2005).
3. Pasumarthi, K.B., Nakajima, H., Nakajima, H.O., Soonpaa, M.H. & Field, L.J. Targeted expression of cyclin D2 results in cardiomyocyte DNA synthesis and infarct regression in transgenic mice. *Circ. Res.* **96**, 110–118 (2005).
4. Nakajima, H., Nakajima, H.O., Tsai, S.C. & Field, L.J. Expression of mutant p193 and p53 permits cardiomyocyte cell cycle reentry after myocardial infarction in transgenic mice. *Circ. Res.* **94**, 1606–1614 (2004).
5. Woo, Y.J. *et al.* Therapeutic delivery of cyclin A2 induces myocardial regeneration and enhances cardiac function in ischemic heart failure. *Circulation* **114**, 1206–213 (2006).
6. Engel, F.B., Hsieh, P.C., Lee, R.T. & Keating, M.T. FGF1/p38 MAP kinase inhibitor therapy induces cardiomyocyte mitosis, reduces scarring, and rescues function after myocardial infarction. *Proc. Natl. Acad. Sci. U. S. A.* **103**, 15546–15551 (2006).
7. Chaudhry, H.W. *et al.* Cyclin A2 mediates cardiomyocyte mitosis in the postmitotic myocardium. *J. Biol. Chem.* **279**, 35858–35866 (2004).
8. Engel, F.B. *et al.* p38 MAP kinase inhibition enables proliferation of adult mammalian cardiomyocytes. *Genes Dev.* **19**, 1175–1187 (2005).